



The role of FeS and $(\text{NH}_4)_2\text{CO}_3$ additives on the pressed type Fe electrode

C.A. Caldas, M.C. Lopes, I.A. Carlos *

Group of Electrochemistry and Polymers, DQ-UFSCar, P.O. Box 676, CEP 13565-905, São Carlos SP, Brazil

Received 5 January 1998; accepted 13 January 1998

Abstract

In the present work the influence of the FeS and $(\text{NH}_4)_2\text{CO}_3$ additives on the Ni–Fe battery negative plate was studied through galvanostatic and potentiostatic discharges. Some aspects of the Fe electrode discharge mechanism in the presence of the FeS were elucidated. The presence of $(\text{NH}_4)_2\text{CO}_3$ as pore forming agent in the Fe electrode was advantageous since it increased the capacity. © 1998 Elsevier Science S.A. All rights reserved.

Keywords: Ni–Fe batteries; Porous electrodes; Passivation; Iron sulfide; Ammonium carbonate

1. Introduction

An increasing interest has been devoted in recent years to the porous iron electrodes of Ni–Fe batteries [1–3]. These electrodes are suitable for applications in traction and stationary batteries, since they have a high theoretical capacity (0.96 A h g^{-1}), long cycle life, low price and a good resistance to mechanical shocks, vibrations, overcharge and deep discharge [4].

However, the porous iron electrode presents a low hydrogen overpotential which limits its application in commercial batteries. The hydrogen evolution occurring on this electrode at open circuit causes the corrosion of the iron electrode and consequently a high autodischarge rate. Furthermore, this electrode presents a low charge efficiency since the hydrogen evolution reaction competes with the discharge reaction [5]. Sulfide salts are used in the iron electrode to improve its performance. Studies show that the addition of both FeS to the electrode's active material [6] and Na_2S to the KOH electrolytic solution [2,7] increases significantly the iron electrode capacity. However, these studies do not clarify the mechanism through which the additives increase the electrode capacity.

Iron electrodes produced recently are of the sintered or pressed type. The pressed type iron electrode costs less to manufacture, but has the disadvantage of lower porosity,

and consequently lower capacity, than the sintered type [1]. The aim of the present research is first to study the effect of FeS on the oxidation reactions (Fe to $\text{Fe}(\text{OH})_2$ and $\text{Fe}(\text{OH})_2$ to $\text{Fe}(\text{III})$) in the pressed type iron electrode, and secondly to study the effect of ammonium carbonate (pore forming agent) on this electrode through galvanostatic and potentiostatic discharge.

2. Experimental procedure

The pressed type iron electrodes used in this work were obtained by hot-pressing a nickel plated steel grid between two equal amounts of a mixture of active material and various additives. Electrolytic iron powder ARMCO (9.9% w/w, $20 \mu\text{m}$, $10 \text{ m}^2 \text{ g}^{-1}$, 0.580 g) was used as active material and the additive was added in the following proportions relating to Fe mass: 6 cg/g low-density polyethylene binder; 5 cg/g graphite; 1 cg/g iron sulfide and ammonium carbonate 10, 20 and 30 cg/g. The pressing process was carried out in the following conditions: compacting pressure 240 kg cm^{-2} ; compacting temperature 112°C and load retention time 3 min. The dimensions of the iron electrodes were $1.2 \text{ cm} \times 1.2 \text{ cm} \times 1.8 \text{ mm}$.

The porosity (P) of iron electrodes was determined by weighing the electrode before and after water absorption by the pores during a certain time (t) [8].

The electrochemical measurements were carried out using a three electrode cell. The counter electrode was

* Corresponding author.

nickel plate. The electrolyte was a 6 M KOH + 0.33 M LiOH solution. Potentials were referred to the Hg/HgO (6 M KOH) reference electrode.

The iron electrodes were initially submitted to galvanostatic stabilization cycles: 26 cycles for electrodes containing FeS and 12 cycles for electrodes without that additive. In each cycle the electrode is charged at 15 mA cm^{-2} (94 mA g^{-1}) for 5 h and discharged at 2 mA cm^{-2} (12 mA g^{-1}) until the potential of -0.70 V was reached.

Potentiostatic discharge was carried out after the iron electrode had been submitted to stabilization cycles. The electrode was maintained for 20 min at a cathodic overpotential of -0.1 V and immediately after, an anodic overpotential in the range between 50 and 270 mV was applied. These overpotentials correspond to the difference between the applied potential and the potential after the electrode has been charged (-1.2 V). For each experiment a new electrode was used. The potentiostatic experiments were considered finished when the charge of the process did not change for a period of 2 h. This value of potentiostatic charge (Q_p) was considered as the maximum charge produced during the potentiostatic discharge [9].

The limit capacity (C_L) and the limit utilization coefficient (β) are given by the following equations [9]:

$$C_L = \frac{Q_p}{w} \quad \text{and} \quad \beta = \frac{Q_p}{Q_t} \quad (1)$$

where w is the mass of active material and Q_t the theoretical charge. The Q_t is given by the equation:

$$Q_t = \frac{nFw}{M} \quad (2)$$

where n is the number of electrons involved in the discharge reaction, F is the Faraday constant and M is the molar mass of the iron.

3. Results and discussion

3.1. General behavior

A triangular sweep voltammetry of the porous pressed type Fe electrode in 6 M KOH + 0.33 M LiOH solution is shown in Fig. 1. The first anodic peak (a_1) at -0.88 V is attributed to oxidation of the Fe to Fe(OH)_2 , while the second anodic peak (a_2) at -0.62 V is attributed to oxidation of the Fe(OH)_2 to Fe(III) [8].

The cyclic voltammogram whose inversion potential was -0.78 V (dashed line) is indicated in this figure. In this voltammogram, the cathodic peak c_1 has disappeared showing that it is related to peak a_2 . Thus, this cathodic peak corresponds to the reduction of Fe(III) to Fe(OH)_2 . The cathodic peak corresponding to reduction of the

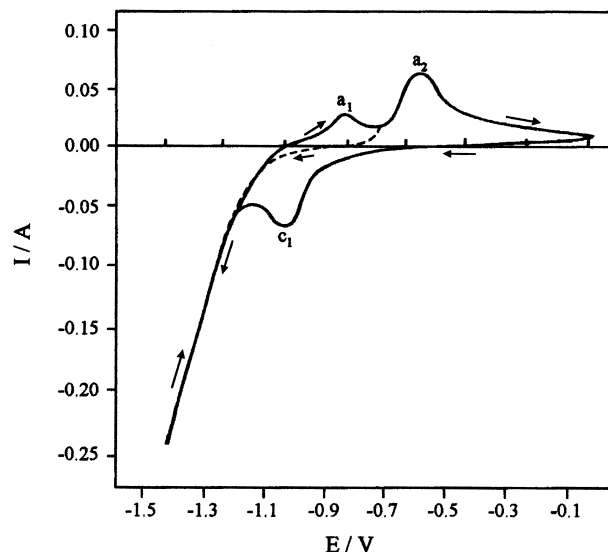


Fig. 1. Triangular sweep voltammetry curves for porous pressed type Fe electrodes. The inversion potential is -0.09 V for full line and -0.78 V for dashed line voltammograms. These curves correspond to the first voltammetry performed in 6 M KOH + 0.33 M LiOH solution at 0.5 mV s^{-1} .

Fe(OH)_2 to Fe is not visible, probably because it was superimposed by the H_2 evolution reaction.

An interesting approach to porous electrodes capacity analysis was suggested by D'alkaine et al. [9]. The authors proposed the evaluation of the percentage of active material utilization by exhaustive potentiostatic discharge. The total capacity obtained by this method is not limited by mass transport and is denominated by limit capacity (C_L). The ratio between limit capacity and active material mass gives the limit utilization coefficient (β).

The same author studied the variation of β for porous PbO_2 electrodes as a function of the potentiostatic discharge overpotential (η) [10,11]. The authors verified that β initially increases up to a maximum and then decreases

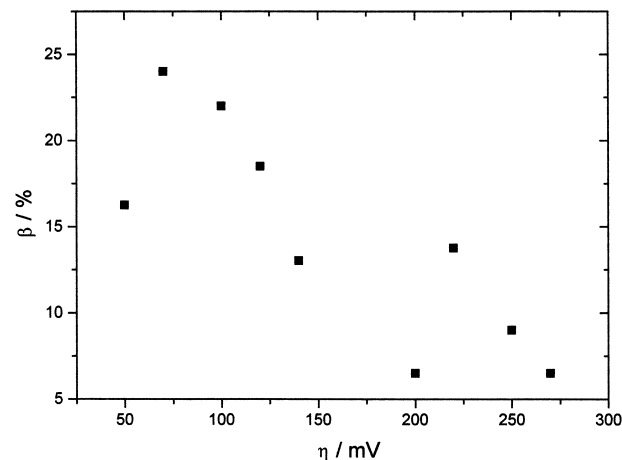


Fig. 2. Limit active material utilization coefficient (β) as function of the potentiostatic discharge overpotential (η) for porous pressed type Fe electrodes in 6 M KOH + 0.33 M LiOH solution.

with overpotential. These facts were explained on the basis of passive film formation. The initial increase in β is expected because the higher the overpotential the greater the free energy disposable for film growth. However, the electric field inside the film also increases with the overpotential and consequently its aging process is faster [10]. This last fact causes the observed decrease in β after the maximum. We applied these ideas to porous pressed type Fe electrodes and obtained the results shown in Fig. 2.

The results in Fig. 2 are in remarkable agreement with the ideas discussed above. The two maximum observed in β correspond to the formation of two different passivating films: $\text{Fe}(\text{OH})_2$ and Fe_3O_4 .

3.2. The role of the FeS

On the basis of the previous discussion, we can relate the FeS additive effect on Fe electrodes to the formation of the passive film.

Fig. 3 shows typical discharge curves for pressed type Fe electrodes in the presence and absence of FeS. Both curves show two plateau, which can be associated with two characteristic oxidation reactions: Fe to $\text{Fe}(\text{OH})_2$ in the first, $\text{Fe}(\text{OH})_2$ to Fe_3O_4 in the second plateau [8]. It is observed that the first plateau is lengthened and shifted to more cathodic potential due to the addition of the FeS, while the second plateau remains unaffected.

Fig. 4 shows the influence of the discharge current density on capacity of pressed type Fe electrodes with different FeS contents. The electrodes with FeS show a marked increase in capacity with respect to the FeS free electrode. This effect was previously reported for the iron electrode [6], nevertheless, it is not completely understood.

In order to explain the facts observed in Figs. 3 and 4, we recall a model that proposes the incorporation of the sulfide ions in $\text{Fe}(\text{OH})_2$ lattice in a way similar to the incorporation of lithium [12]. The sulfide ions' incorpora-

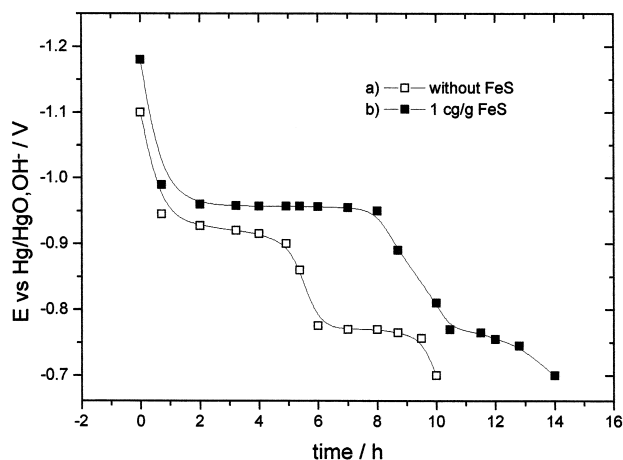


Fig. 3. Typical discharge curves of the pressed type Fe electrode with (a) 0% and (b) 1% of FeS in 6 M KOH + 0.33 M LiOH solution. $i_d = 2 \text{ mA cm}^{-2}$ or 15 mA g^{-1} , 26th cycle.

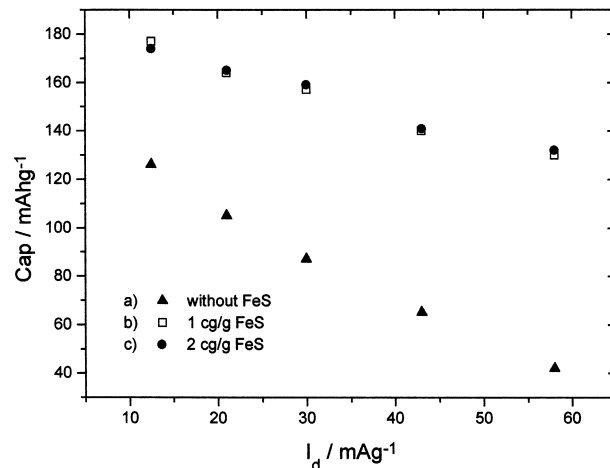


Fig. 4. Capacity as a function of discharge current density for pressed type Fe electrodes with (a) 0% (b) 1% and (c) 2% of FeS in 6 M KOH + 0.33 M LiOH solution.

tion causes a distortion in $\text{Fe}(\text{OH})_2$ structure leading to an increase in defect concentration of the film and consequently, its ionic conductivity rises. Obviously, this retards the passivation process and a thicker film is formed, which explains the lengthening of the first discharge plateau (Fig. 3) and the increase in total capacity (Fig. 4). The shift of the first discharge plateau (Fig. 3) is also explained because a smaller overpotential is required for the electric current to flow through a less resistive film.

The decrease of capacity with increasing current density (Fig. 4) is a widely known result that can be understood on the basis of a passivation film formation: the higher the current density the faster the aging of the film and consequently the smaller its final thickness. Fig. 4 also shows that the fall of the capacity with current density increase is less pronounced for the electrodes containing FeS. This shows that the FeS retards the film aging process. The increase of the FeS content from 1% to 2% does not affect

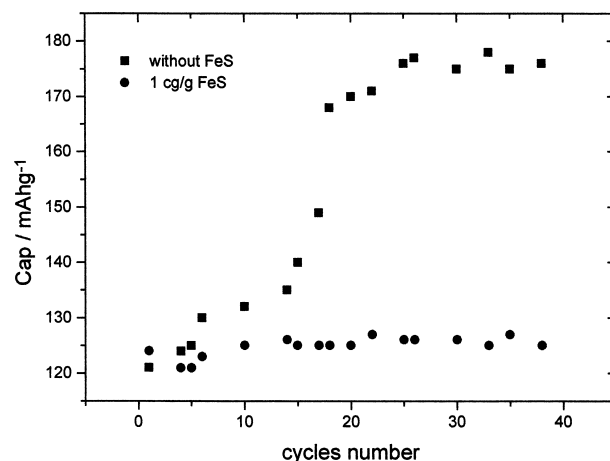


Fig. 5. Capacity values in initial stabilization cycles for porous pressed type Fe electrodes in 6 M KOH + 0.33 M LiOH solution.

Table 1

Porosity values for pressed type Fe electrodes containing 1 cg/g of FeS and different mass percentages of $(\text{NH}_4)_2\text{CO}_3$

$(\text{NH}_4)_2\text{CO}_3$	Porosity
0%	25%
10%	32%
20%	36%
30%	42%

the capacity showing that a limited amount of sulfide ions can be incorporated into the $\text{Fe}(\text{OH})_2$ film.

To account for the observation that the second discharge plateau (Fig. 3) is not affected by the addition of FeS, two explanations are possible: (i) the sulfide ions are hindered by the inner $\text{Fe}(\text{OH})_2$ film and do not arrive at the Fe_3O_4 formed at the film/solution interface; (ii) the presence of substitutional sulfide ions in the Fe_3O_4 lattice does not disturb it significantly, possibly because sulfide and oxygen ions have the same charge. The elucidation of these features requires a more detailed investigation.

In Fig. 5 the capacity in initial stabilization cycles is plotted against the number of cycles. Once again the observed behavior is in agreement with the proposed model. A larger number of stabilization cycles for FeS containing electrodes is necessary for the distribution of the sulfide ions in the Fe electrode surface. The number of 25 stabilization cycles shown in Fig. 5 is in agreement with the reported data for pressed electrodes [6].

3.3. The role of the $(\text{NH}_4)_2\text{CO}_3$

The capacity values shown in Fig. 4 are quite small if compared with sintered type electrodes [3]. This is due to the low porosity of the pressed type electrodes. Since the porosity is low, the area of the active material in contact with the electrolyte is small, which is indicated by the low

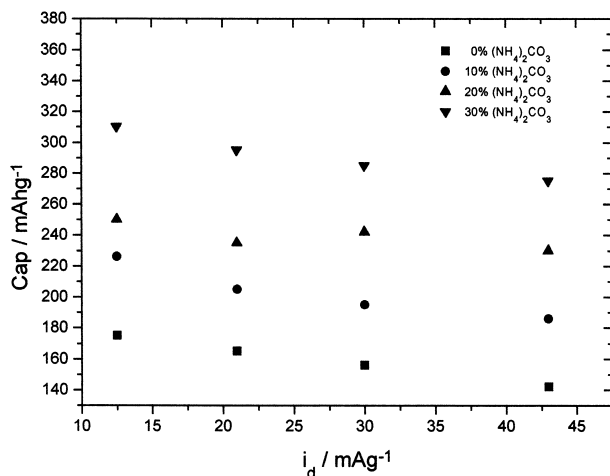


Fig. 6. Capacity as function of discharge current density for pressed type Fe electrodes with 1% of FeS and (■) 0%, (●) 10%, (▲) 20% and (▼) 30% m/m $(\text{NH}_4)_2\text{CO}_3$ in 6 M KOH + 0.33 M LiOH solution.

Table 2

Effect of the addition of the FeS and $(\text{NH}_4)_2\text{CO}_3$ on limit capacity (C_L) and limit active material utilization coefficient (β) of pressed type Fe electrodes

FeS content (%)	Porosity (%)	m_{Fe} (g)	C_L (mA h g^{-1})	β (%)
0	25	0.600	231.5	24.0
1	25	0.602	290.3	30.2
1	42	0.455	354.3	37.0

The values are obtained at the overpotential corresponding to a maximum β value ($\eta = -0.70$ V).

limit active material utilization coefficient shown in Fig. 2 (about 25% at the maximum).

In order to increase the electrode area in contact with the electrolyte, $(\text{NH}_4)_2\text{CO}_3$ is added to the active mass before the pressing process. When the temperature reaches 58°C the $(\text{NH}_4)_2\text{CO}_3$ decomposes into ammonia, carbon dioxide and water according to the following reaction:



The evolution of the NH_3 and CO_2 gases leads to pore formation and consequently, both porosity and surface area of the active material increase. Table 1 shows the influence of different amounts of $(\text{NH}_4)_2\text{CO}_3$, added to the active mass, on the porosity of the Fe electrode.

Clearly the expected result is observed and the corresponding effect on electrode capacity as can be seen in Fig. 6.

The results in Fig. 6 show that the addition of $(\text{NH}_4)_2\text{CO}_3$ increases significantly the pressed type Fe electrode capacity. Addition of $(\text{NH}_4)_2\text{CO}_3$ above 30% is not convenient because the active material was observed to fall out.

The influence of both $(\text{NH}_4)_2\text{CO}_3$ and FeS was studied also through potentiostatic discharge. Table 2 shows these results.

The increase in β and C_L with the addition of $(\text{NH}_4)_2\text{CO}_3$ reflects the increase of the electrode's surface area and confirms the former results. The increase in β and C_L with the addition of FeS occurs because a thicker film is formed over the whole electrode surface area.

4. Conclusions

The role of the FeS in the Fe electrode discharge was interpreted on the basis of the passivation theory. The sulfide ions act principally at the metal/film interface promoting the growth of the $\text{Fe}(\text{OH})_2$ film but not affecting the growth of the Fe_3O_4 film.

The presence of $(\text{NH}_4)_2\text{CO}_3$ in the Fe electrode improves significantly the performance of the pressed type electrode enabling its utilization as an alternative less expensive and technologically more accessible in relation to sintered electrodes.

References

- [1] C. Chakkaravarthy, P. Periasamy, S. Jegannathan, K. Vasu, *J. Power Sources* 35 (1991) 21.
- [2] P. Periasamy, *J. Power Sources* 63 (1996) 79.
- [3] J. Cerny, J. Jindra, K. Micka, *J. Power Sources* 45 (1993) 267.
- [4] S.V. Falk, A.J. Salking, *Alkaline Storage Batteries*, Vol. 1, Wiley, New York, 1969.
- [5] L. Semyonov, *Storage Batteries Maintenance Manual*, Mir Publishers, Moscow, 1977, p. 24.
- [6] K. Vijayamohan, A.K. Shukla, S. Sathyanarayana, *J. Electroanal. Chem.* 289 (1990) 55.
- [7] M. Jayalakshmi, B. Nathira, V.R. Chidmbaram, R. Sabapathi, V.S. Muralidharan, *J. Power Sources* 39 (1992) 113.
- [8] C.A.C. Souza, Ph.D. Thesis, Federal University of São Carlos, Brazil, August 1994.
- [9] C.V. D'alkaine, M.A.S. Santanna, L.A. Avaca, *J. Power Sources* 30 (1990) 153.
- [10] C.V. D'alkaine, M.C. Lopes, Proc. XI CIBAE-IX SIBEE, Aguas de Lindoia, Brasil, 4–9 April 1994, p. IV 16.
- [11] C.V. D'alkaine, M.C. Lopes, *J. Power Sources* 64 (1997) 111.
- [12] J. Cerny, K.K. Micka, *J. Electrochem. Soc.* 123 (1976) 1691.